# Inorganic Materials and Ionic Liquids: Large-scale Nanopatterning of Single Proteins used as Carriers of Magnetic Nanoparticles (Adv. Mater. 5/2010)

**ARTICLE** *in* ADVANCED MATERIALS · FEBRUARY 2010

Impact Factor: 17.49 · DOI: 10.1002/adma.201090008

ADVANCED MATERIALS
www.advmat.de

Materials Views
www.MaterialsViews.com

# Large-scale Nanopatterning of Single Proteins used as Carriers of Magnetic Nanoparticles

By *Ramsés V. Martínez, Javier Martínez, Marco Chiesa, Ricardo Garcia,* Eugenio Coronado,* Elena Pinilla-Cienfuegos,* and *Sergio Tatay*

The development of patterning methods for proteins and other functional molecules onto surfaces with nanoscale accuracy is indispensable to take advantage of their properties in ultra-sensitive and/or high-density devices.[1–5] Several methods to fabricate organized 2D nanostructures make use of the ability of molecules to self-assemble through mutual recognition properties.[6] However, the supramolecular organization attained from "bottom-up" approaches is either difficult to extend from nano- to mesoscopic length scales or does not allow accurate placement of the desired structures on a specific region of an inhomogeneous surface. Similarly, a variety of methods based on Coulomb-force-directed assembly of nanoparticles have been proposed.[7–9] Those methods provide patterning over large areas although the lateral resolution seems limited to above 50 nm. Different "top-down" lithography techniques, such as printing lithography[10–12] or scanning probe-based lithography,[13–20] have demonstrated the ability to pattern functional structures. Template-directed growth or assembly of conjugated materials[18] or iron nanoparticles[19] has been achieved by scanning probe methods. However, tip-based nanofabrication has limitations to pattern large areas. By combining the use of patterned stamps and controlled dewetting[4] the patterning of single molecule magnets, crystalline aggregates of molecular compounds,[21] or nanoparticle superlattices[10] over large areas has been demonstrated. Still, the positioning of single molecules on these nanopatterns with 10 or sub-10 nm resolution remains a challenge. A strategy to overcome the above limitations is to combine "bottom-up" approaches with "top-down" nanolithographic techniques. A viable nanopatterning must also be compatible with the conditions where the molecules preserve their integrity and properties.[22]

An appealing model is provided by ferritin, which is a cage-shaped biomolecule that accommodates an iron oxyhydroxide nanoparticle.[23] The structure of the iron core resembles that of ferrihydrite with a nominal formula $(FeOOH)_8(FeOH_2PO_4)$. This protein is formed by a polypeptidic hollow shell (apoferritin) of ca. 12 nm that encapsulates a ca. 7 nm iron-based core (Fig. 1d). Ferritin is remarkably stable and robust, and is able to withstand not only high temperatures (up to 70 °C), but also wide pH variations. Its isoelectric point is ca. 4.5, so that at pH values below 4.5 it becomes positively charged, while at larger pH values the ferritin is negatively charged. From the chemical point of view, the apoferritin cage can be used as a nanoreactor to synthesize a wide variety of nanoparticles inside, including metal nanoparticles.[24–27] Several methods have been developed or applied to pattern ferritin molecules.[28–31] In most cases, the patterning involved features made of aggregates of ferritin molecules and/or it was restricted to rather small areas.[30]

Here we report a simple yet efficient method to deposit ferritin biomolecules over large areas, with an accuracy that matches the protein size (~10 nm). The selective deposition is driven by the electrostatic interactions existing between the proteins and the nanopatterned surface. The sign of the interaction is controlled by changing the pH of the solution. Magnetic force

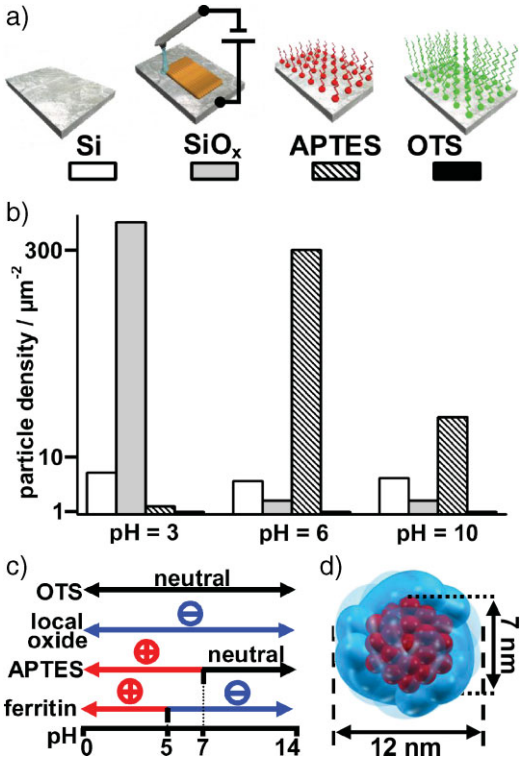


**Figure 1.** Ferritin attachment on the bare, local oxide, OTS, and APTES silicon surfaces as a function of the pH of the solution containing the molecules. a) Scheme of the different surfaces. b) Histograms of the particle density for the different surfaces. c) Summary of the effective surface charge polarization as a function of the pH. d) Scheme of the ferritin size and structure.

[*] Prof. R. Garcia, Dr. R. V. Martínez, Dr. J. Martínez, Dr. M. Chiesa
Instituto de Microelectrónica de Madrid, CSIC
Isaac Newton 8, 28760 Tres Cantos, Madrid (Spain)
E-mail: ricardo.garcia@imm.cnm.csic.es
Prof. E. Coronado, E. Pinilla-Cienfuegos, Dr. S. Tatay
Instituto de Ciencia Molecular (ICMol)
Universidad de Valencia
Polígono de la Coma s/n, 46071 Paterna, Valencia (Spain)
E-mail: eugenio.coronado@uv.es

DOI: 10.1002/adma.200902568

microscopy measurements show that the patterning process does not alter the magnetic properties of the ferritin.

Our study was performed on four different surfaces that have silicon as the bulk substrate (Fig. 1a): i) silicon surfaces Si(100) covered by a very thin layer of native silicon dioxide (ca. 1 nm), ii) silicon dioxide patterns fabricated by local oxidation nanolithography with an atomic force microscopy (AFM), iii) silicon surfaces functionalized with a self-assembled monolayer of octadecyltrichlorosilane (OTS) and iv) self-assembled monolayers of aminopropyltriethoxysilane (APTES) grafted on a silicon surface. In a first step, the different affinities of the surfaces toward the ferritin molecules were tested as a function of the pH of the solution. These experiments were performed by drop-casting 20 μl of a solution of the ferritin molecules at the desired pH for 45 s, then the surface was rinsed in distilled water and blown dry in $N_2$ gas. Under different pH values, the deposition of the ferritin into the above surfaces displays distinct and highly controllable attachment properties. Figure 1b shows the particle density as a function of the pH of the solution containing the ferritin. The quantitative results are derived from the analysis of a series of AFM images (Supporting Information, Fig. S1). At low pH, the molecules are predominantly deposited on the local silicon oxide patterns with a ratio greater than 40:1. At pH = 6 the surface functionalized with APTES becomes favored, reaching a density of about 300 particles per μm. The ratio with respect to the other regions is again 40:1. At higher pH, the preferentiality on the APTES surface decreases, while no major changes are observed on the other surfaces (silicon, local silicon oxide patterns, and OTS-functionalized surface). It is worth noticing that over the range of pH values examined here (from 3 to 10), the ferritin shows little preferentiality for its attachment to the bare and the OTS-functionalized silicon surfaces. The AFM images show, respectively, less than 10 particles per μm and 1 particle per μm for silicon and OTS surfaces.

The above observations can be explained in terms of electrostatic interactions (Fig. 1c). At low pH, the ferritin becomes positively charged and it is repelled by the amino-terminated group, which is protonated at low pH values. At pH = 6, the ferritin is negatively charged so it is attracted by the APTES monolayer, which is still protonated.[28,31] At higher pH, most of the ammonium groups on APTES are neutralized and therefore, the electrostatic attraction between the proteins and the APTES surface is reduced. The local silicon oxide patterns are negatively charged as a consequence of the trapped charges generated during the field-induced oxidation process occurring inside the oxide nanostructure. The trapped charge characterizes the local oxidation process and it does not depend on the pH of the solution containing the proteins. Consequently, at low pH the positively charged ferritin molecules are still attracted toward the local oxide marks.

Similarly, the ferritin molecules can be detached from the surface by changing the pH. For example, the molecules attached to the APTES-functionalized silicon surface are completely removed after sonication for a few seconds in an aqueous solution at pH = 3 (see Supporting Information). This removal process does not alter the properties of the functionalized surface, because new ferritin molecules can be re-deposited at pH = 6 on the same sample surface.

We describe two tip-based nanolithography methods and a printing method developed to pattern ferritin molecules with nanoscale accuracy. The tip-based methods make use of the preferential attachment of ferritin on either local oxides or APTES silicon surfaces shown in the preceding section. AFM nanolithography has fabricated one of the smallest periodic patterns at ambient conditions,[32] so it will be a valuable technique to define the resolution limits of ferritin patterning. Two different pH conditions – acidic and neutral – are designed to deposit the ferritin molecules. Figure 2a schematizes the method followed to deposit ferritin molecules on the local oxide nanopatterns under acidic conditions (pH = 3). The silicon surface is covered with an APTES monolayer and then a region is locally oxidized with the AFM tip. The oxidation process also removes the monolayer under the tip. The nanostripe before deposition is shown in Figure 2b, while Figure 2c shows a densely packed distribution of proteins on the nanostripe. The ferritin molecules form a non-periodic structure with an average molecule–molecule distance of 20 nm (inset in Fig. 2c). The total absence of ferritin molecules outside the patterned stripe is remarkable. This result underlines the strong selectivity of the patterning process. The compositional map provided by the AFM phase image[33] (Fig. 2d and 2e) shows three distinctive materials: the substrate (Si + native oxide), the local oxide, and the molecules.

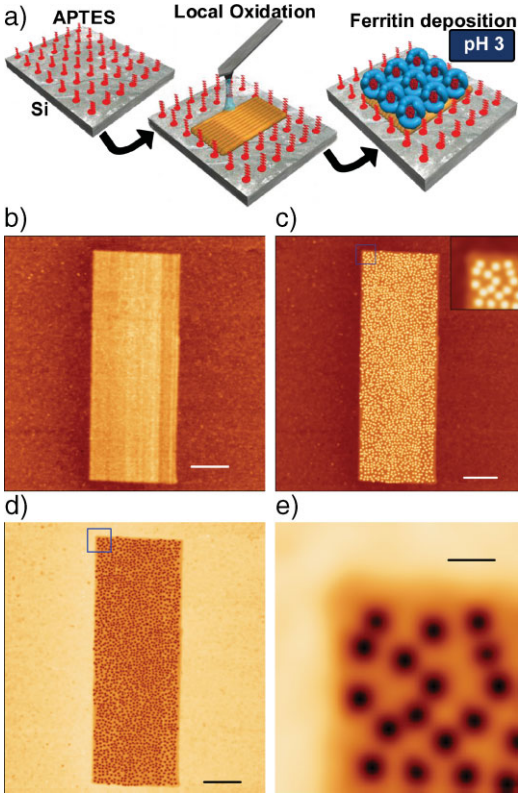


**Figure 2.** Patterning of ferritin molecules by combining local oxidation nanolithography and silicon functionalization at low pH values. a) Scheme of the nanopatterning process. b) AFM image of a local oxide pattern. c) High density packing of ferritin molecules on the local oxide nanopattern. The inset shows the distribution of the proteins in the marked region. d,e) The compositional contrast provided by the AFM phase images reveals three different materials, the bare silicon surface, the local oxide, and the ferritin. (scale bars: 500 nm (b–d), 50 nm (e)).

ADVANCED MATERIALS
www.advmat.de

Materials Views
www.MaterialsViews.com

By increasing the pH from 3 to 6, the ferritin changes its charge from positive to negative. The ferritin interacts repulsively with the local oxide pattern, which prevents its attachment. For this reason, we apply a method based on the combination of OTS-functionalized and APTES-functionalized regions for the attachment of the molecules at pH values above 4.5. The neutral character of an OTS monolayer minimizes the electrostatic interaction with the negatively charged ferritin molecule. Likewise, the ferritin molecules should be strongly attracted to the nanopatterns functionalized with APTES.

The above factors form the basis of the method developed to pattern ferritin at pH values close to 7 (Fig. 3a). The process involves four main steps. First, the silicon surface is functionalized with an OTS monolayer. This replaces OH groups that dominate the native silicon surfaces in air with a methyl-terminated neutral surface. Then, a region of the functionalized surface is locally oxidized. The oxidation process removes the OTS monolayer.[34–36] The sample is immersed in an APTES solution until an APTES monolayer is deposited on the patterned region. The last step involves the deposition of the proteins. The comparison between the nanopattern before and after deposition of the proteins illustrates both the preferentiality and the selectivity of the deposition process (Fig. 3b and 3c). The accuracy of positioning individual ferritin molecules can be determined by patterning an array of parallel lines with a periodicity of 100 nm (Fig. 3d). Each single local oxide line is about 10 nm wide, i.e., very close to the molecule diameter (see inset). A string of ferritin molecules that form 1D arrays can be observed in the narrowest sections of the patterned lines (Fig. 3e). This demonstrates that a single-molecule deposition can be achieved by matching the width of the nanopattern to the molecule size.

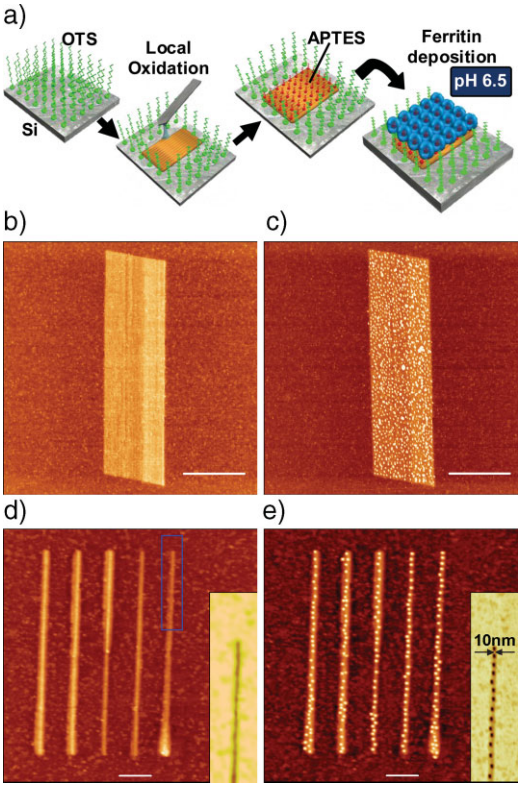


**Figure 3.** Patterning of ferritin molecules by combining local oxidation nanolithography and surface functionalization at pH values close to neutral. a) Scheme of the major steps of the nanopatterning process. b) Local oxide pattern before ferritin deposition. c) AFM image of the distribution of the proteins on the nanopattern. d) Parallel array of narrow local oxide lines. The inset shows the AFM phase image of the marked section of a line. e) Topography AFM image of the five ferritin molecules lines deposited on the 10–15 nm local oxide lines. The inset shows the AFM phase image of a section of a line containing individual ferritin molecules. The ferritin molecules appear as dark spots. (scale bars: 1 μm (b,c), 100 nm (d,e)).

Tip-based oxidation is a sequential process, which has inherent limitations to pattern very large areas. However, the elemental steps investigated by the AFM nanolithography are general and can be extended to pattern ferritin molecules over macroscopic regions. For this application, we use print-based methods such as lithography-controlled dewetting.[4,10] Figure 4a schematizes the process used to form parallel arrays of single ferritin lines covering square-centimeter regions. A soft stamp inked with the molecules is lightly pressed against a silicon surface functionalized with APTES. The formation of a nanoscale liquid meniscus between each protrusion of the soft stamp and the silicon surface functionalized with APTES leads to the selective deposition of ferritin molecules. The lateral size of the meniscus determines the number of molecules deposited per line width. The meniscus size is controlled by the applied load. Figure 4b and 4c show a parallel array of single-molecule ferritin lines. The separation between the ferritin lines matches the periodicity of the protrusions on the stamp ~700 nm. The regularity of the ferritin lines indicates that periodic structures in the sub-100 nm range could be obtained by using stamps with 100 nm or smaller periodicities. The inset in Figure 4c reveals that the size of the object matches the size of the ferritin molecule ~10 nm. These nanopatterns are stable at room temperature and ambient

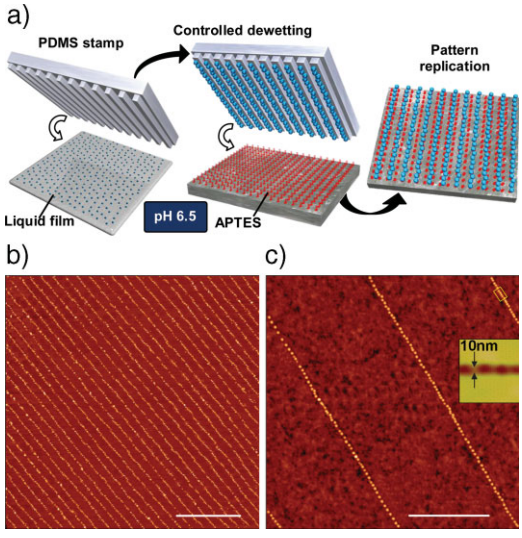


**Figure 4.** Parallel patterning of ferritin molecules obtained by lithography controlled dewetting. a) Scheme of the major steps required to pattern large areas of a silicon surface with nanoscale features made of ferritin molecules. b) Parallel array of single ferritin molecules covering a 1 $cm^2$ region. c) High-resolution AFM image of the single-molecule ferritin lines. The inset shows the line diameter. (scale bars: 5 μm (b), 500 nm (c)).

pressure. Furthermore, magnetic force microscopy measurements performed on aggregates of ferritin molecules deposited by the above methods reveal that the magnetism of the encapsulated iron-core nanoparticle is preserved by the patterning process.

Our results show that the combination of top-down nanolithography techniques and bottom-up electrostatic interactions provides an efficient way to pattern single-molecules of ferritin on silicon surfaces with an accuracy similar to the size of the molecules (~10 nm). Thus, 1D arrays of individual ferritin molecules have been accurately patterned over a sub-micrometer region of the macroscopic silicon surface. In a different experiment, parallel arrays of single-molecule ferritin lines have been patterned over macroscopic silicon surfaces. By tuning the electrostatic interactions between the ferritin and the substrate via the pH, we have shown how this parameter can be used to effectively control the final position of the ferritin molecules, as well as the attachment/detachment process. This soft patterning method does not alter the morphology or the magnetic properties of the deposited molecules, as both topography and magnetic force microscopy experiments reveal. We have also shown that single protein patterning can be achieved with serial and parallel nanolithography. This emphasizes the robustness and general character of the nanolithography principles exposed here. The unprecedented control on the positioning of the biomolecules may open a versatile method to fabricate nanopatterns of functional nanoparticles, using the ferritin molecules as carriers of the nanoparticles.

## Experimental

*Silicon Samples*: The semiconductor samples were p-type Si(100) with a resistivity of 10–12 Ω cm. The silicon surfaces were sonicated three times in a bath of $NH_4OH/H_2O_2/H_2O$ (1:1:2) for 12 min each, then sonicated in deionized water (5 min), and blown dry in $N_2$.

*Ferritin*: Horse spleen ferritin (Type I) was acquired from Fluka Biochemika (Germany). The starting concentration was 85 mg $mL^{-1}$ in a 0.15 M NaCl solution. Here, the starting concentration was diluted in deionized water by mixing 5.8 μL of the starting solution in 20 mL of water. The solution containing the proteins was deposited on the silicon surfaces for 30 s, the sample was then rinsed in deionized water, and blown dry in $N_2$. Acidic ferritin solutions were obtained by mixing the ferritin solution with HCl until the desired pH is obtained. Basic ferritin solutions were obtained by performing the mixing in $NH_4OH$.

*Self-Assembled Monolayers on Silicon*: 3-aminopropyltriethoxylsilane (APTES) at 99% was acquired from Sigma Aldrich and used as received. To prepare a 1 mM solution, 11 μL of the starting solution was mixed with 50 mL of ethanol. A silicon sample was immersed in the solution for 45 min, then rinsed, successively, in ethanol and water. Octadecyltrichlorosilane (OTS) at 90% was acquired from Sigma Aldrich and used as received. To prepare 1 mM solution, 5 μL of the starting solution were mixed with 10 mL of anhydrous toluene. Prior to the functionalization, the silicon surface was heated at 80 °C in a solution of $NH_4OH/H_2O_2/H_2O$ at the ratio 1:1:4 for 30 min. This process assures that the Si surface is OH-terminated. Then, the sample was blown dry with nitrogen and introduced in the OTS solution for 90 s. Next, the OTS-functionalized silicon surface was successively sonicated for 10 min in toluene, chloroform, ethanol, and water. Finally, the surface was blown dry in $N_2$.

## Acknowledgements

This work was financially supported by the Ministerio de Ciencia e Innovación (MAT2006-03833, MAT2007-61584, Consolider-Ingenio in Molecular Nanoscience), the CSIC (PIF2008, TRANSBIO), the European Union (MolSpinQIP), and the Generalidad Valenciana (PROMETEO Program). Supporting Information is available online from Wiley InterScience or from the author.

Received: July 30, 2009
Published online: November 30, 2009

[1] H. Agheli, J. Malmström, E. M. Larsson, M. Textor, D. S. Sutherland, *Nano Lett.* **2006**, *6*, 1165.
[2] M. Geissler, Y. N. Xia, *Adv. Mater.* **2004**, *16*, 1249.
[3] B. D. Gates, Q. B. Xu, M. Stewart, D. Ryan, C. G. Willson, G. M. Whitesides, *Chem. Rev.* **2005**, *105*, 1171.
[4] M. Cavallini, F. Biscarini, S. Leon, F. Zerbetto, G. Bottari, D. A. Leigh, *Science* **2003**, *299*, 531.
[5] Y. Cui, M. T. Bjork, J. A. Liddle, C. Sonnichsen, B. Boussert, A. P. Alivisatos, *Nano Lett.* **2004**, *4*, 1093.
[6] F. J. M. Hoeben, P. Jonkheijm, E. W. Meijer, A. Schenning, *Chem. Rev.* **2005**, *105*, 1491.
[7] H. O. Jacobs, S. A. Campbell, M. G. Steward, *Adv. Mater.* **2002**, *14*, 1553.
[8] C. R. Barry, J. Gu, H. O. Jacobs, *Nano Lett.* **2005**, *5*, 2078.
[9] C. F. Chen, S. D. Tzeng, M. H. Lin, S. Gwo, *Langmuir* **2006**, *22*, 7819.
[10] W. L. Cheng, N. Y. Park, M. T. Walter, M. R. Hartman, D. Luo, *Nat. Nanotechnol.* **2008**, *3*, 682.
[11] M. Cavallini, I. Bergenti, S. Milita, G. Ruani, I. Salitros, Z. R. Qu, R. Chandrasekar, M. Ruben, *Angew. Chem. Int. Ed.* **2008**, *47*, 8596.
[12] A. Zeira, D. Chowdhury, R. Maoz, J. Sagiv, *ACS Nano* **2008**, *2*, 2554.
[13] S. Krämer, R. R. Fuierer, C. B. Gorman, *Chem. Rev.* **2003**, *103*, 4367.
[14] R. Garcia, R. V. Martinez, J. Martinez, *Chem. Soc. Rev.* **2006**, *35*, 29.
[15] M. Liu, N. A. Amro, G. Y. Liu, *Annu. Rev. Phys. Chem.* **2008**, *59*, 367.
[16] S. T. Liu, R. Maoz, J. Sagiv, *Nano Lett.* **2004**, *4*, 845.
[17] L. Seemann, A. Stemmer, N. Naujoks, *Nano Lett.* **2007**, *7*, 3007.
[18] R. Garcia, M. Tello, J. F. Moulin, F. Biscarini, *Nano Lett.* **2004**, *4*, 1115.
[19] Y. H. Wang, W. Wei, D. Maspoch, J. S. Wu, V. P. Dravid, C. A. Mirkin, *Nano Lett.* **2008**, *8*, 3761.
[20] M. Cavallini, C. Albonetti, F. Biscarini, *Adv. Mater.* **2009**, *21*, 1043.
[21] E. M. Puchner, S. K. Kufer, M. Strackharn, S. W. Stahl, H. E. Gaub, *Nano Lett.* **2008**, *8*, 3692.
[22] M. Mannini, F. Pineider, P. Sainctavit, C. Danieli, E. Otero, C. Sciancalepore, A. M. Talarico, M. A. Arrio, A. Cornia, D. Gatteschi, R. Sessoli, *Nat. Mater.* **2009**, *8*, 194.
[23] P. M. Harrison, P. Arosio, *Biochim. Biophys. Acta* **1996**, *1275*, 161.
[24] S. Gider, D. D. Awschalom, T. Douglas, S. Mann, M. Chaparala, *Science* **1995**, *268*, 77.
[25] H. Yoshimura, *Colloid Surf. A* **2006**, *282*, 464.
[26] N. Galvez, P. Sanchez, J. M. Dominguez-Vera, A. Soriano-Portillo, M. Clemente-Leon, E. Coronado, *J. Mater. Chem.* **2006**, *16*, 2757.
[27] M. Clemente-Leon, E. Coronado, A. Soriano-Portillo, N. Galvez, J. M. Dominguez-Vera, *J. Mater. Chem.* **2007**, *17*, 49.
[28] I. Yamashita, *Thin Solid Films* **2001**, *393*, 12.
[29] S. Yoshii, K. Yamada, N. Matsukawa, I. Yamashita, *Jpn. J. Appl. Phys.* **2005**, *44*, 1518.
[30] S. Kumagai, S. Yoshii, K. Yamada, N. Matsukawa, I. Fujiwara, K. Iwahori, I. Yamashita, *Appl. Phys. Lett.* **2006**, *88*, 153103.
[31] T. Yoshinobu, J. Suzuki, H. Kurooka, W. C. Moon, H. Iwasaki, *Electrochim. Acta* **2003**, *48*, 3131.
[32] R. V. Martinez, N. S. Losilla, J. Martinez, Y. Huttel, R. Garcia, *Nano Lett.* **2007**, *7*, 1846.
[33] R. Garcia, R. Magerle, R. Perez, *Nat. Mater.* **2007**, *6*, 405.
[34] H. Sugimura, N. Nakagiri, *Langmuir* **1995**, *11*, 3623.
[35] J. W. Zheng, Z. H. Zhu, H. F. Chen, Z. F. Liu, *Langmuir* **2000**, *16*, 4409.
[36] D. Wouters, R. Willems, S. Hoeppener, C. F. J. Flipse, U. S. Schubert, *Adv. Funct. Mater.* **2005**, *15*, 938.